

# Fluid Antenna Multiple Access Assisted Integrated Data and Energy Transfer: Outage and Multiplexing Gain Analysis

Xiao Lin, Yizhe Zhao, *Member, IEEE*, Halvin Yang, Jie Hu, *Senior Member, IEEE*, Kai-Kit Wong, *Fellow, IEEE*

**Abstract**—Fluid antenna multiple access (FAMA) exploits the spatial opportunities in wireless channels to overcome multiuser interference by position (a.k.a. port) switching, which can achieve better performance compared to traditional fixed multiple-input multiple-output (MIMO) systems. Additionally, integrated data and energy transfer (IDET) is capable of providing both wireless data transfer (WDT) and wireless energy transfer (WET) services towards low-power devices. In this paper, a FAMA-assisted IDET system is investigated, where a base station (BS) equipped with  $N$  fixed antennas provides dedicated IDET services towards  $N$  user equipments (UEs). Each UE is equipped with a single fluid antenna, while the power splitting (PS) approach is conceived for coordinating WDT and WET. The outage probabilities of both WDT and WET are derived and approximated into closed-forms, where the fluid antenna (FA) at each UE selects the optimal port to achieve the maximum signal-to-interference-plus-noise ratio (SINR) or the energy harvesting power (EHP). The IDET outage probabilities are defined and subsequently derived and approximated into closed-forms. Further, multiplexing gains of the proposed system are defined and analyzed to evaluate the performance. Numerical results validate the theoretical analysis, while also illustrate that the trade-off is achieved between WDT and WET performance by exploiting different port selection strategies. Furthermore, the number of UEs should be optimized to achieve better IDET performance of the system.

**Index Terms**—Fluid antenna system, fluid antenna multiple access (FAMA), integrated data and energy transfer (IDET), outage probability, multiplexing gain.

## I. INTRODUCTION

The rapid advances in mobile communications technology mean that massive low-power devices are swarming into the networks for providing a variety of services to smart factories and smart cities, etc. [1], [2]. It is posing formidable challenges to energy supplement for such devices as manually charging or replacing batteries entails additional human costs, a main bottleneck in many applications [3]. Integrated data and energy transfer (IDET) has been envisioned to address the battery life issues for low-power devices in next-generation wireless networks [4]. Usually, devices have both data and energy requirements, and thus wireless data transfer (WDT) and wireless energy transfer (WET) should be coordinated at the transceiver, which yields the concept of IDET [5], [6].

Traditional multiple input multiple output (MIMO) technology enhances the performance of IDET systems in congested

networks using of spatial multiplexing, diversity coding, and beamforming techniques [7], [8]. However, MIMO is usually associated with increased energy consumption and hardware costs, with the need of multiple antennas and radio frequency (RF) chains, which is often impractical for low-power devices under limited hardware resources. To address these challenges, fluid antenna (FA) has emerged in recent years as a promising solution for future wireless communication systems [9], [10]. A FA system (FAS) represents the general concept of shape-flexible and position-flexible antenna technologies which may be implemented adopting surface wave technology [11] and reconfigurable pixels [12]. The latter can achieve near-zero-delay switching of antenna position for communications. It is anticipated that FAS has great potential in IDET systems.

Regarding IDET systems, the received signals often suffer from serious power attenuation in the transmission path, which will degrade the IDET efficiency, especially for WET, whose activating power threshold is much higher than that of WDT [13]. Hence, to glean sufficient energy for functioning reliably, FAS can be useful in providing higher IDET efficiency with a much smaller hardware size compared to traditional fixed-position MIMO technology. Specifically, the spatial diversity gain from FA can significantly enhance the capability of low-power devices to achieve better performance in both WDT and WET, which is more suitable for an IDET system.

### A. Related Work

In most research results, WDT and WET are coordinated by one of the two common approaches, namely, time switching (TS) and power splitting (PS) [5], [6]. In the TS approach, a time switch is applied at the receiver to allow user equipments (UEs) to perform information decoding (ID) or energy harvesting (EH) in different time slots. By contrast, in the PS approach, a power splitter at the UE is utilized to divide the received signal into two parts, one for ID and another for EH. Results for the TS approach and the PS approach have been reported in various wireless systems, such as broadcast channel (BC) [14], cooperative non-orthogonal multiple-access (NOMA) network [15], interference channels (IFCs) [16], [17], [18] and etc. Specifically, Lee *et al.* considered a two-user IDET multiple-input single-output (MISO) BC with a new joint TS approach [14], and Kurup *et al.* then investigated an adaptive power allocation scheme for the IDET-enabled cooperative NOMA network under the TS approach [15]. Also, [16] introduced a novel precoding design, while [17] proposed beamforming designs, ensuring both Quality-of-Service (QoS) and the EH constraints in the MISO channel. Furthermore, [18] addressed the joint design of transmit beamforming with

Xiao Lin, Yizhe Zhao and Jie Hu are with the School of Information and Communication Engineering, University of Electronic Science and Technology of China, Chengdu 611731, China. (e-mail: xiaolin@std.uestc.edu.cn; yzzhao@uestc.edu.cn; hujie@uestc.edu.cn).

Halvin Yang and Kai-Kit Wong are with the Department of Electronic and Electrical Engineering, University College London, WC1E 7JE London, U.K. (e-mail: uceehy@ucl.ac.uk; kai-kit.wong@ucl.ac.uk). K. K. Wong is also affiliated with Yonsei Frontier Lab, Yonsei University, Korea.

either PS ratios or transmit TS ratios in a multicell network. Moreover, Zhao *et al.* proposed a novel time index modulation assisted IDET system, where data is delivered not only by the phase-amplitude modulation but also by the multiple activated time indices for either WDT or WET [19], [20].

On the other hand, FAS research is comparatively a newer endeavor. The use of FAS for wireless communications was first proposed by Wong *et al.* in 2020 [21], [22]. Subsequently, results have been presented on the performance of FAS for single-user communication, focusing on the outage probability and diversity gain [23], [24], [25], [26]. A two-stage approximation incorporating more parameters into the channel model was proposed in [23], offering a more accurate characterization of the performance for FAS. In [24], the authors simplified the outage probability at high signal-to-noise ratio (SNR) and obtained the diversity gain of FAS. By combining space-time rotations with code diversity, Psomas *et al.* designed space-time coded modulations which attain promising performance over block-fading channels [25]. Later in [26] and [27], the authors used an asymptotic matching method to analyze the performance of FAS under Nakagami fading channels. Other work also studied the performance of FAS under  $\alpha$ - $\mu$  fading channels [28] and considered the continuous FAS where the change of position can be infinitely fine [29]. Most recently, the MIMO-FAS setup where both ends have FAS with multiple activated ports was also investigated in [30].

FAS is more than just a new degree of freedom for design and optimization. In [31], [32], [33], it was shown that position flexibility enabled by FAS can simplify multiple access and allow spectrum sharing on the same physical channel without precoding and without interference cancellation. The approach in [31], [32] is dubbed as fast fluid antenna multiple access (FAMA) which switches antenna position at each UE on a per-symbol basis to mitigate inter-user interference. Fast FAMA is powerful but is not known practically achievable. By contrast, the slow FAMA scheme in [33] is more practical as it only requires each UE to switch its FA port once in each channel coherence time. In [34], the performance of the two-user slow FAMA channel was accurately studied while [35] adopted the Gauss-Laguerre and Gauss-Hermite quadrature to conduct the performance analysis applicable to any number of UEs. Deep learning has also been utilized to reduce the burden of signal-to-interference-plus-noise ratio (SINR) observation at the ports [36]. Later in [37], the authors developed an optimal stochastic control algorithm based on mean-field game theory to address the power control problem in the slow FAMA system. Besides, the advantages of opportunistic scheduling in FAMA systems were characterized in [38]. Advanced system models involving FAS such as integrated sensing and communication (ISAC) [39], dirty multiple access channels [40] and NOMA [41] have also been considered. There is also a branch of FAS under the name ‘movable antenna’ that focuses on the implementation using stepper motors and has generated interesting results. A list of recent work can be found in [42].

## B. Motivation and Contributions

Overall, however, there are few works studying FAMA (or FAS) assisted IDET. In our previous work [43], we analyzed

the outage probabilities for WDT and WET in a slow FAMA-assisted IDET system, where the TS approach was conceived. It was evaluated that FAMA assisting IDET is able to achieve better WDT and WET performance, when compared to the traditional MIMO assisted IDET system [44], [45]. In general, existing results showed that the PS approach always achieves better IDET performance than the TS approach, which requires accurate synchronization between transmitters and receivers. To the best of our knowledge, the integration of FAS into IDET systems with the PS approach remains unexplored. In the PS approach, port selection strategy simultaneously affects both the WDT and WET, making performance analysis more challenging compared to that of the TS approach, where WDT and WET can be segregated into different time slots.

In this paper, our aim is to investigate the FAMA-assisted IDET systems considering the application of the PS approach for coordinating WDT and WET at the UEs. Throughout, slow FAMA is always assumed, and each UE switches its FA to the most desirable port, obtaining either the maximum SINR or the maximum energy harvesting power (EHP). We concentrate on investigating the outage probabilities and multiplexing gains for WDT and WET based on these two strategies. Additionally, in order to provide a more comprehensive view of the performance of the proposed system, the special IDET outage probability, general IDET outage probability, special IDET multiplexing gain and general IDET multiplexing gain are defined and analyzed by simultaneously considering both WDT and WET. Specifically, our contributions are summarized as follows:

- This paper investigates the FAMA-assisted IDET system using PS to coordinate WDT and WET, where each UE is equipped with a single  $K$ -port FA. Each UE is able to dynamically select the optimal receive port according to various WDT and WET requirements.
- The outage probabilities of WDT and WET are analyzed by considering different port selection strategies. Specifically, we derive the exact WDT and WET outage probabilities with the WDT oriented strategy for maximizing the SINR and the WET oriented strategy for maximizing the EHP. Afterwards, the WDT outage probability with the WDT oriented strategy and the WET outage probability with the WET oriented strategy are approximated in closed forms, respectively. Further, the WDT and WET multiplexing gains are defined and analyzed.
- Both the special and general IDET outage probabilities are analyzed without considering a specific port selection strategy, thereby offering a more comprehensive view of the proposed system. Then the IDET outage probabilities are approximated in closed forms. Furthermore, the special multiplexing IDET gain and the general IDET multiplexing gain are defined and analyzed.
- Simulation results validate the theoretical analysis of the FAMA-assisted IDET system and provide some novel insights for the system design.

The rest of this paper is organized as follows. Section II introduces the system model of the FAMA-assisted IDET system. In Section III, the outage probabilities and multiplex-

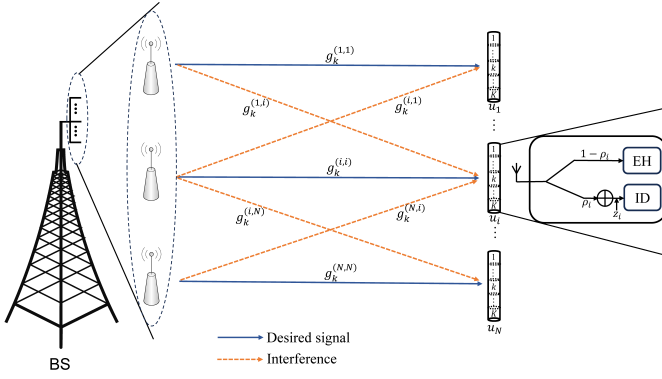


Fig. 1: A FAMA assisted IDET system.

ing gains for WDT and WET with different port selection strategies are analyzed, which is followed by the performance analysis of IDET in Section IV. After providing simulation results in Section V, we conclude this paper.

## II. SYSTEM MODEL

Consider a downlink FAMA-assisted IDET system consisting of a base station (BS) equipped with  $N$  fixed antennas and  $N$  UEs. Each UE is equipped with a  $K$ -port linear FA having the size of  $W\lambda$ , where  $W$  represents the normalized size of FA and  $\lambda$  denotes the wavelength. It is assumed that each BS antenna is dedicated to communicating with its corresponding UE, *i.e.*, the  $i$ -th BS antenna communicates with UE  $i$ , and each UE uses the PS approach to coordinate WDT and WET, as shown in Fig. 1. The UEs may also receive the interference signals from other BS antennas, which may degrade the WDT performance but provide more signal sources for WET.

### A. Wireless channel model

The wireless channel gain between the  $m$ -th BS antenna and the  $k$ -th port of UE  $i$  is characterized by [33]

$$g_k^{(m,i)} = \left( \sqrt{1 - \mu^2} x_k^{(m,i)} + \mu x_0^{(m,i)} \right) + j \left( \sqrt{1 - \mu^2} y_k^{(m,i)} + \mu y_0^{(m,i)} \right), \quad (1)$$

where  $x_0^{(m,i)}, \dots, x_K^{(m,i)}$  and  $y_0^{(m,i)}, \dots, y_K^{(m,i)}$  are independent Gaussian random variables with zero mean and variance of 1. Note that the correlation among different ports is realized by invoking the same variables  $x_0^{(m,i)}, y_0^{(m,i)}$ . Also,  $\mu$  represents the correlation parameter among different ports, which can be chosen by [33]

$$\mu = \sqrt{2} \sqrt{{}_1F_2 \left( \frac{1}{2}; 1, \frac{3}{2}; -\pi^2 W^2 \right) - \frac{J_1(2\pi W)}{2\pi W}}, \quad (2)$$

where  ${}_aF_b(\cdot; \cdot; \cdot)$  denotes the generalized hypergeometric function and  $J_1(\cdot)$  is the first-order Bessel function of the first kind.

### B. IDET with PS approach

UE  $i$  applies the PS approach to coordinate WDT and WET from the received signal. Specifically, the received signal at

each UE is split for the WDT and WET by a power splitter, which divides  $\rho_i$  ( $0 \leq \rho_i \leq 1$ ) portion of the signal power for WDT, and the remaining  $1 - \rho_i$  portion of power for WET. Each UE is assumed to have its own requirements for the SINR of WDT and the EHP of WET. Then, the received signal split for WDT by activating the  $k$ -th port is expressed as

$$y_{k,i}^{\text{WDT}} = \underbrace{\sqrt{\rho_i} \sqrt{\frac{P_i}{d_i^\beta}} g_k^{(i,i)} s_i}_{\text{desired signal by } i\text{-th BS antenna}} + \underbrace{\sum_{m \neq i} \sqrt{\rho_i} \sqrt{\frac{P_m}{d_m^\beta}} g_k^{(m,i)} s_m}_{\text{interference caused by the rest BS antennas}} + \underbrace{\sqrt{\rho_i} \eta_k^i + z_i}_{\text{noise}}, \quad (3)$$

where  $s_i$  is the transmit Gaussian signal for UE  $i$ ,  $P_i$  denotes the transmission power of  $s_i$ ,  $d_i$  and  $d_m$  represent the distance from the  $i$ -th BS antenna to UE  $i$  and the distance from the interfering  $m$ -th BS antenna to UE  $i$ , and  $\beta$  represents the path loss exponent. Moreover,  $\eta_k^i$  is the complex additive white Gaussian noise (AWGN) with zero mean and variance of  $\sigma_\eta^2$  at the  $k$ -th port of UE  $i$ , and  $z_i$  is the passband-to-baseband noise of UE  $i$ , which also follows the complex Gaussian distribution with zero mean and variance of  $\sigma_c^2$ . Accordingly, the received SINR at  $k$ -th port of UE  $i$  is given by

$$\begin{aligned} \text{SINR}_k^i &= \frac{\rho_i \frac{P_i}{d_i^\beta} |g_k^{(i,i)}|^2 \mathbb{E}[\|s_i\|^2]}{\rho_i \sum_{m \neq i} \frac{P_m}{d_m^\beta} |g_k^{(m,i)}|^2 \mathbb{E}[\|s_m\|^2] + (\rho_i \sigma_\eta^2 + \sigma_c^2)} \\ &\stackrel{(a)}{\approx} \frac{\rho_i \frac{P_i}{d_i^\beta} |g_k^{(i,i)}|^2}{\rho_i \sum_{m \neq i} \frac{P_m}{d_m^\beta} |g_k^{(m,i)}|^2} \\ &\stackrel{(b)}{=} \frac{|g_k^{(i,i)}|^2}{\sum_{m \neq i} |g_k^{(m,i)}|^2}, \end{aligned} \quad (4)$$

where (a) assumes that the interference power is much greater than the noise power, and the SINR is reduced to the signal-to-interference-ratio (SIR), (b) assumes the case that all the BS antennas have identical transmit power  $P^1$  and all the distances from the BS antennas to UE  $i$  is the same ( $d_i = d, \forall i$ ).<sup>2</sup>

The signal split for WET at UE  $i$  by activating the  $k$ -th port is expressed as

$$y_{k,i}^{\text{WET}} = \sqrt{1 - \rho_i} \left( \sum_{m=1}^N \sqrt{\frac{P_m}{d_m^\beta}} g_k^{(m,i)} s_m + \eta_k^i \right). \quad (5)$$

Then, the EHP for WET at UE  $i$  by activating the  $k$ -th port is given by

$$Q_k^i = (1 - \rho_i) \frac{P}{d^\beta} \sum_{m=1}^N |g_k^{(m,i)}|^2. \quad (6)$$

<sup>1</sup>Since we focus on the performance analysis of the FAMA-assisted IDET system but not the power allocation among BS antennas, it is assumed that all the BS antennas have identical transmit power  $P$  for analytical tractability.

<sup>2</sup>Since the distance between the BS and the UEs is much farther than the antennas spacing, the differences among antenna-UE pairs are neglected.

### III. WDT AND WET PERFORMANCE ANALYSIS WITH DIFFERENT PORT SELECTION STRATEGIES

In this section, we will study the outage probabilities for WDT and WET by conceiving different port selection strategies in the FAMA-assisted IDET system. The multiplexing gains for WDT and WET will also be analyzed.

#### A. Port selection strategy

The interference signals at each UE may result in different impact on the performance of WDT and WET. For instance, a stronger interference may cause ID failure but might increase the EHP for WET. Consequently, the FA can adjust the port selection strategy to maximize the SINR or the EHP to meet various requirements. On the one hand, if UE  $i$  is more eager to achieve better WDT performance, it applies the WDT oriented port selection strategy, where the UE chooses an optimal port that maximizes the SINR in (4), which is given by

$$k_{\text{SINR}}^* = \arg \max_k \frac{|g_k^{(i,i)}|^2}{\sum_{m \neq i}^N |g_k^{(m,i)}|^2} \triangleq \arg \max_k \frac{X_k}{Y_k}, \quad (7)$$

where

$$X_k = \left( x_0^{(i,i)} + \frac{\mu}{\sqrt{1-\mu^2}} x_0^{(i,i)} \right)^2 + \left( y_0^{(i,i)} + \frac{\mu}{\sqrt{1-\mu^2}} y_0^{(i,i)} \right)^2 \quad (8)$$

and

$$Y_k = \sum_{\substack{m=1 \\ m \neq i}}^N \left( x_k^{(m,i)} + \frac{\mu}{\sqrt{1-\mu^2}} x_0^{(m,i)} \right)^2 + \left( y_k^{(m,i)} + \frac{\mu}{\sqrt{1-\mu^2}} y_0^{(m,i)} \right)^2. \quad (9)$$

On the other hand, if UE  $i$  is more eager to achieve a better WET performance, it will apply the WET oriented port selection strategy, where the UE selects an optimal antenna port that maximizes the EHP in (6), which is given by

$$k_{\text{EHP}}^* = \arg \max_k \sum_{m=1}^N |g_k^{(m,i)}|^2 \triangleq \arg \max_k (1-\mu^2)(X_k + Y_k). \quad (10)$$

#### B. Outage probabilities analysis with WDT oriented port selection strategy

It is considered that ID suffers from a failure and WDT experiences an outage if the received SINR at UE  $i$  is lower than a certain threshold  $\gamma$ . Using the port selection strategy in (7), we can analyze the outage probabilities of WDT and WET with the WDT oriented strategy, respectively. Firstly, the WDT outage probability is defined as

$$\epsilon_{\text{WDT-SINR}}^i = \text{Prob} \left( \max_k \text{SINR}_k^i = \frac{X_k}{Y_k} < \gamma \right). \quad (11)$$

According to [33], the exact expression for the WDT outage probability  $\epsilon_{\text{WDT-SINR}}^i$  with the WDT oriented strategy of UE  $i$  is formulated as (12) (see top of next page), where  $(t)_k = t(t+1) \cdots (t+k-1)$  is the Pochhammer symbol [46]. However, (12) is difficult to gain insight. In order to obtain its approximate closed-form solution, we first introduce the approximation method outlined in Lemma 1 below.

**Lemma 1.** Given  $|x| < 1$  and  $|\alpha x| \ll 1$ , we have the binomial approximation as

$$(1+x)^\alpha \approx 1 + \alpha x. \quad (13)$$

*Proof:* The function  $f(x) = (1+x)^\alpha$ , where  $x$  and  $\alpha$  are either real or complex, can be reformulated as a Taylor series about the zero point as

$$f(x) = 1 + \alpha x + \frac{\alpha(\alpha-1)}{2!} x^2 + \cdots. \quad (14)$$

If  $|x| < 1$  and  $|\alpha x| \ll 1$ , then the latter terms in the series become progressively smaller and can be truncated to give the approximation in (13), which concludes the proof. ■

Using Lemma 1, we have the following theorem.

**Theorem 1.** The WDT outage probability with the WDT oriented strategy for maximizing SINR is approximated as

$$\epsilon_{\text{WDT-SINR}}^i \approx \left[ 1 - K \left( \frac{\mu^2}{\gamma+1} \right)^{N-1} - K\mathcal{C} \right]^+, \quad (15)$$

where

$$\mathcal{C} = \left( \frac{2\gamma(1-\mu^2)+1}{2\gamma^2+(3-\mu^2)\gamma+1} \right)^{N-1} (1-\mu^2) \sum_{k=0}^{N-2} \sum_{j=0}^{N-k-2} \frac{(\gamma+1)^{k+1} \gamma^j \binom{N-j-k-1}{j}}{j! [(1-\mu^2)\gamma+1]^{j+k+1}} \quad (16)$$

and  $(a)^+ = \max(0, a)$ .

*Proof:* See Appendix A. ■

**Corollary 1.** As  $K \rightarrow \infty$ , the WDT outage probability goes to 0.

The results in (12) and (15) provide exact and approximated expressions for the WDT outage probability with the WDT oriented strategy of the FAMA-assisted IDET system, respectively. In what follows, we investigate the WET outage, which is defined as the event that the EHP at UE  $i$  falls below a certain threshold  $Q_{\text{th}}$ . To start with, we define

$$\begin{aligned} \hat{Q}_k^i &= \sum_{m=1}^N \left[ \left( x_k^{(m,i)} + \frac{\mu}{\sqrt{1-\mu^2}} x_0^{(m,i)} \right)^2 + \left( y_k^{(m,i)} + \frac{\mu}{\sqrt{1-\mu^2}} y_0^{(m,i)} \right)^2 \right] \\ &= X_k + Y_k. \end{aligned} \quad (17)$$

Using the port selection strategy in (7), the WET outage



$$\begin{aligned} \epsilon_{\text{WDT-SINR}}^i &= \int_0^\infty \int_0^\infty \frac{\tilde{r}^{N-2} e^{-\frac{r+\tilde{r}}{2}}}{2^N \Gamma(N-1)} \left\{ Q_{N-1} \left( \sqrt{\frac{\mu^2 \gamma \tilde{r}}{(1-\mu^2)(\gamma+1)}}, \sqrt{\frac{\mu^2 r}{(1-\mu^2)(\gamma+1)}} \right) - \exp \left( -\frac{\mu^2 (\gamma \tilde{r} + r)}{2(1-\mu^2)(\gamma+1)} \right) \right. \\ &\quad \times \left. \left( \frac{1}{\gamma+1} \right)^{N-1} \sum_{k=0}^{N-2} \sum_{j=0}^{N-k-2} \frac{(N-j-k-1)_j}{j!} \left( \frac{r}{\tilde{r}} \right)^{\frac{j+k}{2}} (\gamma+1)^k \gamma^{\frac{j-k}{2}} I_{j+k} \left( \frac{\mu^2 \sqrt{\gamma r \tilde{r}}}{1-\mu^2 \gamma+1} \right) \right\}^K dr d\tilde{r} \end{aligned} \quad (12)$$

$$\begin{aligned} \epsilon_{\text{WET-SINR}}^i &= K \int_{r_1=0}^\infty \int_{r_2=0}^\infty \int_{z=0}^\infty \int_{y=0}^{\hat{Q}_{\text{th}}} \frac{r_2^{N-2} \exp(-\frac{r_1+r_2}{2})}{2^N \Gamma(N-1)} \left[ Q_1 \left( \sqrt{\frac{\mu^2}{1-\mu^2}} r_1, \sqrt{yz} \right) - Q_1 \left( \sqrt{\frac{\mu^2}{1-\mu^2}} r_1, \hat{Q}_{\text{th}} \right) \right] \times \\ &\quad \frac{1}{2} \left( \frac{y}{\frac{\mu^2}{1-\mu^2} r_2} \right)^{\frac{N-2}{2}} e^{-\frac{y+\frac{\mu^2}{1-\mu^2} r_2}{2}} I_{N-2} \left( \sqrt{\frac{\mu^2}{1-\mu^2}} r_2 y \right) \mathcal{D}(r_1, r_2, z) dy dz dr_1 dr_2 \end{aligned} \quad (19)$$

probability with the WDT oriented strategy is then given by

$$\begin{aligned} \epsilon_{\text{WET-SINR}}^i &= \text{Prob} \left( Q_k^i < Q_{\text{th}} \mid k^* = \arg \max_k \text{SINR}_k^i = \frac{X_k}{Y_k} \right) \\ &= \text{Prob} \left( X_{k^*} + Y_{k^*} < \hat{Q}_{\text{th}} \mid k^* = \arg \max_k \frac{X_k}{Y_k} \right) \\ &= \frac{\text{Prob} \left( X_{k^*} + Y_{k^*} < \hat{Q}_{\text{th}}, k^* = \arg \max_k \frac{X_k}{Y_k} \right)}{\text{Prob} \left( k^* = \arg \max_k \frac{X_k}{Y_k} \right)} \quad (18) \\ &= K \text{Prob} \left( X_{k^*} + Y_{k^*} < \hat{Q}_{\text{th}}, k^* = \max_k \frac{X_k}{Y_k} \right) \\ &= K \text{Prob} \left( Y_{k^*} \max_{n \neq k^*} \frac{X_n}{Y_n} < X_{k^*} < \hat{Q}_{\text{th}} - Y_{k^*} \right), \end{aligned}$$

where  $\hat{Q}_{\text{th}} = \frac{d^\beta Q_{\text{th}}}{(1-\mu^2)(1-\rho_i)P}$ .

Next, we present the exact WET outage probability with the WDT oriented strategy in Theorem 2 below.

**Theorem 2.** *The WET outage probability with the WDT oriented strategy for maximizing the SINR is expressed as (19) (see top of this page), where*

$$\begin{aligned} \mathcal{D}(r_1, r_2, z) &= (K-1) \left[ 1 - \frac{1}{2} \int_0^\infty Q_1 \left( \sqrt{\frac{\mu^2}{1-\mu^2}} r_1, \sqrt{zy} \right) \right. \\ &\quad \times e^{-\frac{y+\frac{\mu^2}{1-\mu^2} r_2}{2}} I_{N-2} \left( \sqrt{\frac{\mu^2}{1-\mu^2}} \sqrt{r_2 y} \right) dy \Big]^{K-2} \times \\ &\quad \int_0^\infty \frac{y^{\frac{N}{2}}}{4 \left( \frac{\mu^2}{1-\mu^2} r_2 \right)^{\frac{N-2}{2}}} e^{-\frac{(z+1)y+\frac{\mu^2}{1-\mu^2}(r_1+r_2)}{2}} \times \\ &\quad I_0 \left( \sqrt{\frac{\mu^2}{1-\mu^2}} r_1 z y \right) I_{N-2} \left( \sqrt{\frac{\mu^2}{1-\mu^2}} r_2 y \right) dy. \end{aligned} \quad (20)$$

*Proof:* See Appendix B. ■

*C. Analysis of WET outage probabilities with different port selection strategies*

In what follows, we investigate the outage probabilities of WET and WDT with the WET oriented strategy for maximizing the EHP. Using the port selection strategy in (10), the WET outage probability is then expressed as

$$\begin{aligned} \epsilon_{\text{WET-EHP}}^i &= \text{Prob} \left( \max_k Q_k^i < Q_{\text{th}} \right) \\ &= \text{Prob} \left( \max_k \hat{Q}_k^i = X_k + Y_k < \hat{Q}_{\text{th}} \right). \end{aligned} \quad (21)$$

According to [43], the WET outage probability with the WET oriented strategy is expressed by

$$\begin{aligned} \epsilon_{\text{WET-EHP}}^i &= \int_0^\infty \frac{r^{N-1} \exp(-\frac{r}{2})}{2^N \Gamma(N)} \times \\ &\quad \left[ 1 - Q_N \left( \sqrt{\frac{\mu^2}{1-\mu^2}} r, \sqrt{\hat{Q}_{\text{th}}} \right) \right]^K dr. \end{aligned} \quad (22)$$

Similarly, we approximate (22) using the same technique as in Lemma 1, which is presented in Theorem 3.

**Theorem 3.** *The WET outage probability with the WET oriented strategy for maximizing the EHP is approximated as*

$$\begin{aligned} \epsilon_{\text{WET-EHP}}^i &\approx \left[ 1 - K \frac{\Gamma \left( N, \frac{\hat{Q}_{\text{th}}}{2} \right)}{\Gamma(N)} \right. \\ &\quad \left. - K \frac{\mu^2 \left( \frac{\hat{Q}_{\text{th}}}{2} \right)^N \exp \left( -\frac{\hat{Q}_{\text{th}}}{2} \right)}{N!} \right. \\ &\quad \left. \times \sum_{l=0}^{N-1} (1-\mu^2)^l {}_1F_1 \left( l+1; N+1; \frac{\mu^2 \hat{Q}_{\text{th}}}{2} \right) \right]^+, \end{aligned} \quad (23)$$

where  $\Gamma(\cdot, \cdot)$  is the upper incomplete gamma function.

*Proof:* See Appendix C. ■

**Corollary 2.** *As  $K \rightarrow \infty$ , the WET outage probability goes to 0.* ■

$$\begin{aligned} \epsilon_{\text{WDT-EHP}}^i &= K \int_{r_1=0}^{\infty} \int_{r_2=0}^{\infty} \int_{y=0}^{\infty} \int_{t=0}^{\gamma y} \frac{r_2^{N-2} \exp\left(-\frac{r_1+r_2}{2}\right)}{2^N \Gamma(N-1)} \left[ 1 - Q_N \left( \sqrt{\frac{\mu^2}{1-\mu^2}} (r_1+r_2), \sqrt{t+y} \right) \right]^{K-1} \times \\ &\quad \frac{1}{2} \exp\left(-\frac{\frac{\mu^2}{1-\mu^2} r_1 + t}{2}\right) I_0\left(\sqrt{\frac{\mu^2}{1-\mu^2}} r_1 t\right) \times \frac{1}{2} \left(\frac{y}{\frac{\mu^2}{1-\mu^2} r_2}\right)^{\frac{N-2}{2}} e^{-\frac{y+\frac{\mu^2}{1-\mu^2} r_2}{2}} I_{N-2}\left(\sqrt{\frac{\mu^2}{1-\mu^2}} r_2 y\right) dt dy dr_1 dr_2 \end{aligned} \quad (25)$$

Next, we investigate the WDT outage probability with the WET oriented strategy for maximizing the EHP. Using the port selection strategy in (7), the WDT outage probability is then found as

$$\begin{aligned} \epsilon_{\text{WDT-EHP}}^i &= \text{Prob}\left(\text{SINR}_{k^*}^i = \frac{X_{k^*}}{Y_{k^*}} < \gamma | k^* = \arg \max_k \widehat{Q}_k^i\right) \\ &= \frac{\text{Prob}\left(\frac{X_{k^*}}{Y_{k^*}} < \gamma, k^* = \arg \max_k X_k + Y_k\right)}{\text{Prob}(k^* = \arg \max_k X_k + Y_k)} \\ &= K \text{Prob}\left(\frac{X_{k^*}}{Y_{k^*}} < \gamma, k^* = \arg \max_k X_k + Y_k\right) \\ &= K \text{Prob}\left(\frac{X_{k^*}}{Y_{k^*}} < \gamma, X_{k^*} + Y_{k^*} \geq \max_{n \neq k^*} X_n + Y_n\right) \\ &= K \text{Prob}\left(\max_{n \neq k^*} X_n + Y_n - Y_{k^*} < X_{k^*} < \gamma Y_{k^*}\right). \end{aligned} \quad (24)$$

Next, we present the WDT outage probability with the WET oriented strategy in Theorem 4.

**Theorem 4.** *The WDT outage probability with the WET oriented strategy for maximizing the EHP is given by (25) (see top of this page).*

*Proof:* See Appendix D. ■

#### D. Analysis of multiplexing gain for WDT and WET

According to [33], the WDT multiplexing gain of the FAMA-assisted IDET system is defined as

$$m_{\text{WDT}} = N (1 - \epsilon_{\text{WDT-SINR}}^i). \quad (26)$$

Here, each BS antenna is assumed to transmit at a constant rate, and ID is successfully performed with the probability of  $(1 - \epsilon_{\text{WDT-SINR}}^i)$ . It is also assumed that all the UEs are statistically identical and have the same SINR threshold.

Similarly, we can define the WET multiplexing gain as

$$m_{\text{WET}} = N (1 - \epsilon_{\text{WET-EHP}}^i), \quad (27)$$

which adopts similar assumptions as in (26).

## IV. IDET PERFORMANCE ANALYSIS

In this section, we conduct theoretical analysis of the IDET outage probabilities and multiplexing gains of the FAMA-assisted IDET system without specific port selection strategy, which reveals the best-effort IDET performance. Two kinds of IDET outage probabilities are defined as follows.

**Special IDET outage probability:** If both WDT and WET suffer from an outage, then IDET suffers from a special outage, indicating that the received SINR and EHP at all the ports are both lower than their respective thresholds. Then, the special IDET outage probability is formulated as

$$\begin{aligned} \epsilon_{\text{IDET-special}}^i &= \text{Prob}\left(\text{SINR}_k^i < \gamma, Q_k^i < Q_{\text{th}}, \forall k = 1, 2, \dots, K\right) \\ &= \text{Prob}\left(\frac{X_k}{Y_k} < \gamma, X_k + Y_k < \widehat{Q}_{\text{th}}, \forall k = 1, 2, \dots, K\right) \\ &= \text{Prob}\left(\frac{X_k}{\gamma} < Y_k < \widehat{Q}_{\text{th}} - X_k, \forall k = 1, 2, \dots, K\right). \end{aligned} \quad (28)$$

Next, we present the expression for the special IDET outage probability in Theorem 5 as follows.

**Theorem 5.** *The special IDET outage probability is formulated in (29) (see top of next page).*

*Proof:* See Appendix E. ■

We have provided an accurate expression for evaluating the IDET outage probability in Theorem 5. Nonetheless, the expression is hard to handle. In order to approximate it into a closed form, we first introduce Lemma 2 below.

**Lemma 2.** *As the parameter  $\mu \rightarrow 0$ , the variables  $\frac{X_k}{Y_k}$  and  $X_k + Y_k$  are approximately independent.*

*Proof:* As  $\mu \rightarrow 0$ ,  $X_k$  and  $Y_k$  can be approximated as following central chi-squared distributions with 2 degrees of freedom and  $2(N-1)$  degrees of freedom, respectively, i.e.,

$$X_k \stackrel{\mu \rightarrow 0}{\approx} (x_0^{(i,i)})^2 + (y_0^{(i,i)})^2, \quad (30)$$

$$Y_k \stackrel{\mu \rightarrow 0}{\approx} \sum_{m \neq i}^N \left[ (x_k^{(m,i)})^2 + (y_k^{(m,i)})^2 \right]. \quad (31)$$

Since the distribution of  $(x_0^{(m,i)}, \dots, x_K^{(m,i)}, y_0^{(m,i)}, \dots, y_K^{(m,i)})$  is radially symmetric, then the ratio

$$\frac{X_k}{Y_k} = \frac{X_k / (X_k + Y_k)}{Y_k / (X_k + Y_k)} \quad (32)$$

has the same distribution as

$$\frac{S_1^2 + S_2^2}{S_3^2 + \dots + S_{2N}^2}, \quad (33)$$

where the vector  $(S_1, \dots, S_{2N})$  is uniformly distributed on a unit sphere in  $\mathbb{R}^{2N}$ . Hence, the variable  $\frac{X_k}{Y_k}$  is independent of  $X_k + Y_k$ , which concludes the proof. ■

Afterwards, by applying Lemma 2, the special IDET outage

$$\begin{aligned} \epsilon_{\text{IDET-special}}^i &= \int_{r_1=0}^{\infty} \int_{r_2=0}^{\infty} \frac{r_2^{N-2} \exp\left(-\frac{r_1+r_2}{2}\right)}{2^N \Gamma(N-1)} \left\{ \int_{x=0}^{\frac{\hat{Q}_{\text{th}}}{(1+1/\gamma)}} \left[ Q_{N-1} \left( \sqrt{\frac{\mu^2}{1-\mu^2}} r_1, \sqrt{\frac{x}{\gamma}} \right) - Q_{N-1} \left( \sqrt{\frac{\mu^2}{1-\mu^2}} r_1, \sqrt{\hat{Q}_{\text{th}} - x} \right) \right] \right. \\ &\quad \left. \times \frac{1}{2} e^{-\frac{x + \frac{\mu^2}{1-\mu^2} r_2}{2}} I_0 \left( \sqrt{\frac{\mu^2}{1-\mu^2}} r_2 x \right) dx \right\}^K dr_1 dr_2 \end{aligned} \quad (29)$$

probability is formulated as

$$\begin{aligned} \epsilon_{\text{IDET-special}}^i &= \text{Prob} \left( \max_k \frac{X_k}{Y_k} < \gamma, \max_k X_k + Y_k < \hat{Q}_{\text{th}} \right) \\ &\stackrel{\mu \rightarrow 0}{\approx} \text{Prob} \left( \max_k \frac{X_k}{Y_k} < \gamma \right) \text{Prob} \left( \max_k X_k + Y_k < \hat{Q}_{\text{th}} \right) \\ &= \epsilon_{\text{WDT-SINR}}^i \epsilon_{\text{WET-EHP}}^i, \end{aligned} \quad (34)$$

where  $\epsilon_{\text{WDT-SINR}}^i$  is accurately derived in (12) and approximated in Theorem 1, while  $\epsilon_{\text{WET-EHP}}^i$  is accurately derived in (22) and approximated in Theorem 3. Thus,  $\epsilon_{\text{IDET-special}}^i$  and  $\epsilon_{\text{IDET-General}}^i$  can also be approximated in closed forms.

**Corollary 3.** For small  $N$ , the special IDET outage probability can be further simplified as

$$\epsilon_{\text{IDET-special}}^i \approx \epsilon_{\text{WDT-SINR}}^i, \quad (35)$$

while for large  $N$ , the special IDET outage probability can be further simplified as

$$\epsilon_{\text{IDET-special}}^i \approx \epsilon_{\text{WET-EHP}}^i. \quad (36)$$

*Proof:* See Appendix F. ■

**General IDET outage probability:** If either WDT or WET suffers from an outage, then the system suffers from a general IDET outage, indicating that no ports can be selected to satisfy both the WDT and WET requirements, which is described by

$$\begin{aligned} \epsilon_{\text{IDET-general}}^i &= \text{Prob} \left( \left\{ \max_k \text{SINR}_k^i < \gamma \right\} \cup \left\{ \max_k Q_k^i < Q_{\text{th}} \right\} \right) \quad (37) \\ &\stackrel{(a)}{=} \epsilon_{\text{WDT-SINR}}^i + \epsilon_{\text{WET-EHP}}^i - \epsilon_{\text{IDET-special}}^i. \end{aligned}$$

where (a) uses the addition law of probability. Similarly, since  $\epsilon_{\text{WDT-SINR}}^i$  is derived in (12) and approximated in Theorem 1,  $\epsilon_{\text{WET-EHP}}^i$  is derived in (22) and approximated in Theorem 3, and  $\epsilon_{\text{IDET-special}}^i$  is derived in Theorem 5 and approximated in (34),  $\epsilon_{\text{IDET-general}}^i$  can be approximated in closed form.

Similarly, the IDET multiplexing gain for the special case and the general case are analyzed as

$$m_{\text{IDET-special}} = N(1 - \epsilon_{\text{IDET-special}}^i), \quad (38)$$

$$m_{\text{IDET-general}} = N(1 - \epsilon_{\text{IDET-general}}^i), \quad (39)$$

where we have assumed that each BS antenna transmits at a constant rate. It is also assumed that all UEs are statistically identical, sharing the same SINR and EHP thresholds.

TABLE I: Parameter Settings

Parameter	Description	Values
$d$	The distance between BS antennas and UEs	10 m [47]
$\beta$	Path loss exponent	2
$P$	Transmit power at BS antennas	1 W
$N$	Number of UEs	5
$K$	Number of ports of a single fluid antenna	200 [33]
$W$	Normalized size of fluid antenna	5 [33]
$\rho$	Power splitting ratio	0.5
$\gamma$	SINR threshold	3 dB [33]
$Q_{\text{th}}$	EHP threshold	10 mW

## V. NUMERICAL RESULTS

In this section, the performance of the FAMA-assisted IDET system is evaluated by both the theoretical analysis and Monte-Carlo simulations. It is assumed that the wireless channels of different BS antenna-UE pairs exhibit identical statistical characteristics. In all our simulations, the markers represent the simulation results, while the curves represent the theoretical results. Unless specifically stated otherwise, the system parameters are set based on the figures in TABLE I.

Figs. 2 to 4 illustrate the outage probabilities versus the number  $N$  of BS antenna-UE pairs. Specifically, Fig. 2 depicts the WDT outage probability with the WDT oriented port selection strategy for maximizing the SINR, the WET outage probability with the WET oriented port selection strategy for maximizing the EHP, as well as the IDET outage probabilities without port selection strategy, where the exact WDT outage probability and the exact WET outage probability are obtained from (12) and (22), respectively. The exact special IDET outage probability and the exact general IDET outage probability are derived in (29) and (37), respectively. It is seen that the derived analytical results match the simulations very well, which validates our theoretical analysis. As the number of BS antenna-UE pairs  $N$  increases, the WET outage probability drops, since the UEs can receive more wireless signals from other BS antennas and further glean more energy. By contrast, the WDT outage probability increases due to more interference from other BS antennas. Besides, we see that the special IDET outage probability converges with the WDT outage probability when  $N$  is small, *i.e.*,  $N = 4$ , while converges with the WET outage probability when  $N$  is large, *i.e.*,  $N = 7$ . This is in line with Corollary 3, where  $\epsilon_{\text{IDET-special}}^i \approx \epsilon_{\text{WDT-SINR}}^i$  for small  $N$  and  $\epsilon_{\text{IDET-special}}^i \approx \epsilon_{\text{WET-EHP}}^i$  for large  $N$ . Conversely, the general IDET probability shows a convex trend with respect to the number  $N$  of BS antenna-UE pairs. A trade-off between

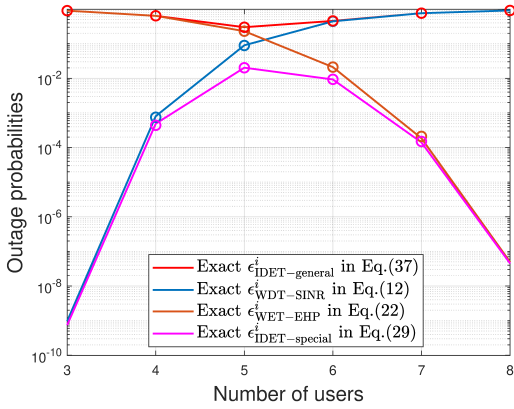


Fig. 2: Outage probabilities versus the number  $N$  of BS antenna-UE pairs.

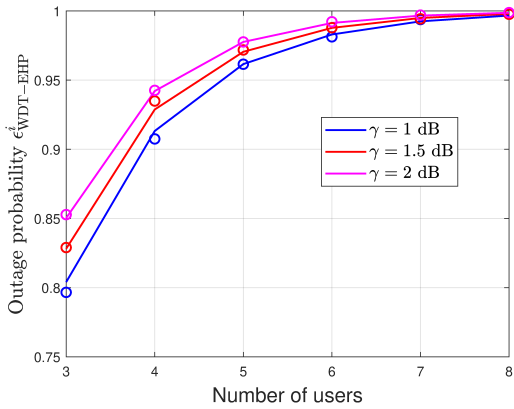


Fig. 3: Exact WDT outage probability with the WET oriented strategy versus the number  $N$  of BS antenna-UE pairs.

the WDT and WET can be achieved by optimizing the number of UEs.

Fig. 3 demonstrates the exact WDT outage probability with the WET oriented port selection strategy for maximizing the EHP versus  $N$ , while Fig. 4 depicts the exact WET outage probability with the WDT oriented port selection strategy for maximizing the SINR versus  $N$ , where different thresholds,  $\gamma$ ,  $Q_{th}$  are conceived, respectively. It is observed that both WDT and WET exhibit poor performance by considering the undesired strategies. This is because when the UEs aim to maximize the SINR via port selection, FAMA tunes into the windows of opportunity where interference naturally disappears in a deep fade, resulting in the lowest EHP. Similarly, when the UEs aim to maximize the EHP via port selection, FAMA tunes into the windows of opportunity with the highest interference, leading to poor performance of WDT. Moreover, higher thresholds impose more stringent requirements for both WDT and WET, resulting in performance degradation.

The multiplexing gains are presented in Fig. 5 and Fig. 6 to investigate the performance of the FAMA-assisted IDET system versus the number  $N$  of BS antenna-UE pairs. It is set that the SINR threshold is  $\gamma = 3$  dB and the EHP threshold is  $Q_{th} = 14$  mW. Specifically, Fig. 5 illustrates that the WDT multiplexing gain is concave with respect to the number  $N$

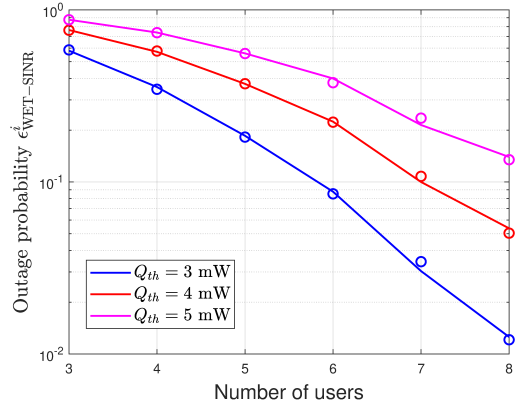


Fig. 4: WET outage probability with the WDT oriented strategy versus the number  $N$  of BS antenna-UE pairs.

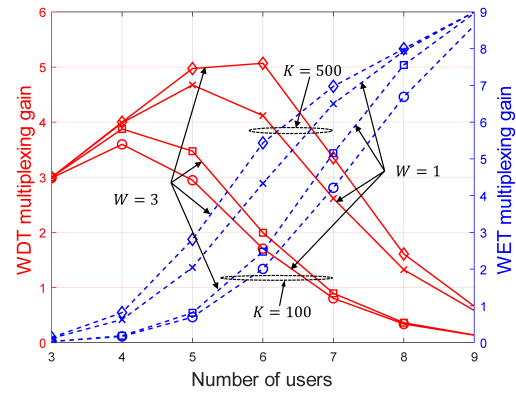


Fig. 5: Multiplexing gain of WDT and WET versus the number  $N$  of BS antenna-UE pairs.

of BS antenna-UE pairs, while the WET multiplexing gain is a strictly increasing function of  $N$ . This is because when we increase  $N$ , the WET outage probability reduces, as seen in Fig. 2. According to (27), the WET multiplexing gain increases with  $N$ . However, as for WDT, a larger  $N$  indicates a much higher WDT outage probability, which then reduces the WDT multiplexing gain. Moreover, as shown in Fig. 6, the special IDET multiplexing gain displays an increase-decrease-increase trend with respect to  $N$  when  $K = 100$ . This is in line with Corollary 3, where  $\epsilon_{IDET-special}^i \approx \epsilon_{WDT-SINR}^i$  for small  $N$  and  $\epsilon_{IDET-special}^i \approx \epsilon_{WET-EHP}^i$  for large  $N$ . Therefore, the special IDET multiplexing gain firstly shows the same concave trend as the WDT multiplexing gain, then shows the same monotonically increasing trend as the WET multiplexing gain. However, for the case with  $K = 500$ , the special IDET multiplexing gain strictly increases with  $N$ . This is because both the WDT and WET outage probabilities are very small, and therefore the multiplexing gains are mainly determined by  $N$ . As expected, the general IDET multiplexing gain shows a concave trend with respect to the value of  $N$ .

Next, Fig. 7 depicts the outage probabilities versus the SINR threshold,  $\gamma$ . Specifically, Fig. 7 illustrates the WDT outage probability with the WDT oriented port selection strategy for maximizing the SINR, as well as the IDET outage probabilities



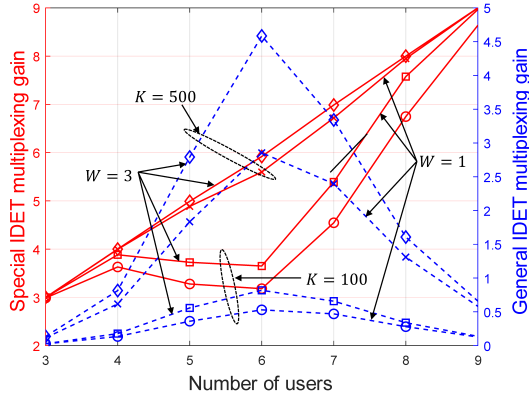


Fig. 6: IDET multiplexing gain versus the number  $N$  of BS antenna-UE pairs.

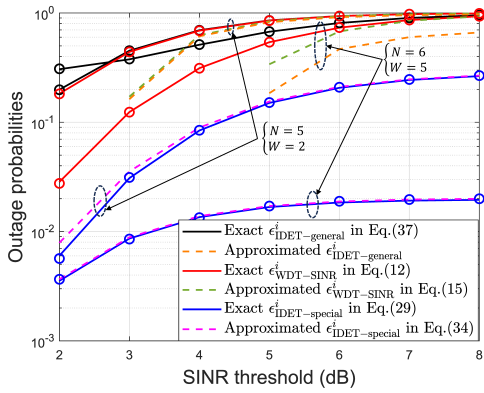


Fig. 7: Outage probabilities versus the SINR threshold  $\gamma$ .

without port selection strategy, where different number  $N$  of BS antenna-UE pairs and fluid antenna size  $W$  are conceived. As shown in Fig. 7, the derived approximated closed-form for WDT outage probability closely approximates the theoretical value, when the SINR threshold is relatively high, *i.e.*,  $\gamma = 4$  dB. The approximated closed-form expression for general IDET is more accurate at  $N = 5$  and  $W = 2$ . This is because as  $N$  decreases,  $Q_N(\cdot)$  also decreases, making  $(1 - Q_N(\cdot))^K$  closer to  $1 - KQ_N(\cdot)$ . Consequently, the approximation of  $\epsilon_{\text{WET-EHP}}$  in (23) is more accurate, leading to a more precise closed-form expression for general IDET. Additionally, the approximated closed-form for special IDET outage probability is more accurate when  $W$  is larger, *i.e.*,  $W = 6$ . This is because the correlation parameter among different ports  $\mu$  is smaller with a higher  $W$ , thereby making it more consistent with the conditions suitable for the approximation in (34).

Fig. 8 depicts the outage probabilities versus the EHP threshold,  $Q_{\text{th}}$ . Specifically, Fig. 8 illustrates the WET outage probability with the WET oriented port selection strategy for maximizing the EHP, as well as the IDET outage probabilities versus  $Q_{\text{th}}$  by conceiving different port number  $K$ . It is expected that the WET and IDET outage probabilities increase with the EHP threshold  $Q_{\text{th}}$ . In addition, as depicted in Fig. 8, the derived approximated closed-forms for WET outage probability in (23) and for general IDET outage probability in (37) closely approximate the exact value, when the EHP threshold

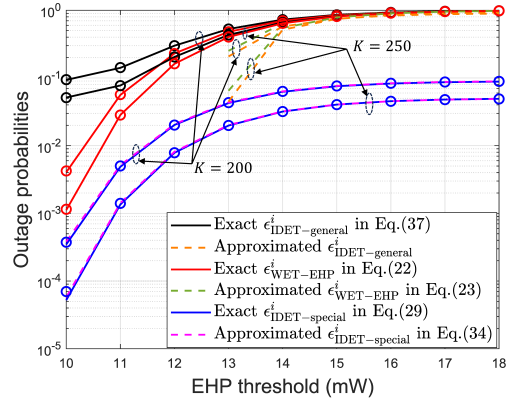


Fig. 8: Outage probabilities versus the EHP threshold  $Q_{\text{th}}$ .

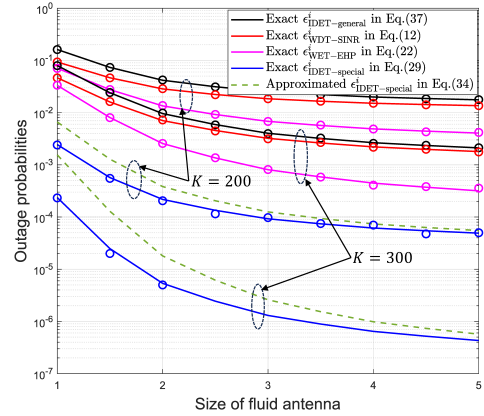


Fig. 9: Outage probabilities versus the fluid antenna size  $W$ .

is relatively high, *i.e.*,  $Q_{\text{th}} = 14$  mW. Furthermore, we observe from Fig. 8 that a larger port number  $K$  concurrently improves both the WET and IDET performance. This is because a larger  $K$  increases the likelihood of selecting an optimal port for having a stronger wireless channel gain, which enhances the received signal strength for IDET.

To explore the effect of fluid antenna size,  $W$  on the outage probabilities of the FAMA-assisted IDET system, we provide the results in Fig. 9 by setting the SINR threshold as  $\gamma = 2$  dB and for different port number  $K$ . As expected, Fig. 9 illustrates that the outage probabilities decrease with the fluid antenna size  $W$ . Besides, when  $W$  is small, *i.e.*,  $W = 1$ , the outage probability becomes unacceptably large, indicating that FAMA is not efficient anymore. It is also seen that when the fluid antenna size  $W$  is small, the performance of IDET improves significantly with  $W$  (from  $W = 1$  to  $W = 3$ ). However, when  $W$  becomes larger, the performance improvement of the IDET system tends to flatten when we increase  $W$  (from  $W = 3$  to  $W = 5$ ). This indicates that an appropriate fluid antenna size  $W$  should be determined by considering the performance improvement as well as the hardware size. Additionally, as  $W$  gradually increases, the approximation of the special IDET outage probability in (34) tends to approach its exact value, since the correlation among different ports is decreasing by increasing  $W$ . Also, a larger port number  $K$  results in a larger approximation error. This is because by increasing  $K$ , the

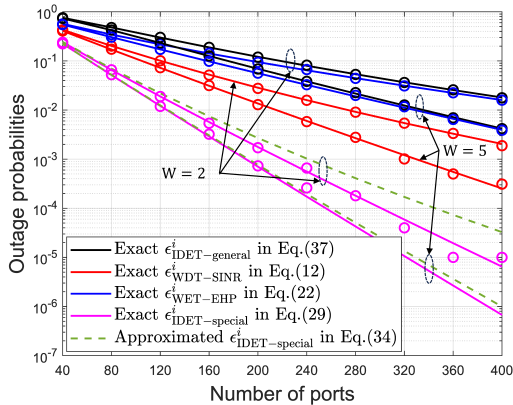


Fig. 10: Outage probabilities versus the number of ports  $K$ .

spatial correlation among different ports gradually increases, which results in a weaker independence assumption.

To further evaluate the effect of port number  $K$  on the performance of the FAMA assisted IDET system, Fig. 10 depicts the outage probabilities versus  $K$  by considering two different fluid antenna size  $W$ . As expected, the performance of the proposed system improves with a larger  $K$  or  $W$ . This is because a larger  $K$  provides more opportunities to select the optimal ports that can reduce interference or strengthen the EHP, while a larger  $W$  reduces the spatial correlation among ports and provides a higher spatial diversity gain.

## VI. CONCLUSION

In this paper, the novel FAMA-assisted IDET system has been investigated by employing the PS approach, where each UE is equipped with a single FA to mitigate multiuser interference or enhance the receive signal strength for energy harvesting by dynamically switching the antenna ports. Specifically, the exact outage probabilities for WDT and WET with different port selection strategies were derived and approximated in closed forms, while the special and general IDET outage probabilities were also analyzed to evaluate the joint IDET performance of the FAMA system. The multiplexing gains for WDT, WET and IDET were also provided to explore the potential system performance. Simulation results validated our theoretical analysis and evaluated the performance of the proposed system providing insights for the FAMA assisted IDET system design, *e.g.*, both WDT and WET exhibit poor performance by considering the undesired strategies.

### APPENDIX A PROOF OF THEOREM 1

As  $\gamma$  increases, the value  $\{\dots\}^K$  in (12) gradually decreases, indicating that Lemma 1 can be used for further approximation. Then the exact WDT outage probability with the WDT oriented strategy for maximizing the SINR in (12) can be approximated as

$$\epsilon_{\text{WDT}}^i \approx (1 - K)\beta_1 + K\beta_2 - K\beta_3, \quad (\text{A.1})$$

where  $\beta_1$  and  $\beta_2$  are defined in [33, eq. (74)] and [33, eq. (75)], respectively, given by

$$\beta_1 = \int_0^\infty \int_0^\infty \frac{\tilde{r}^{N-2} e^{-\frac{r+\tilde{r}}{2}}}{2^N \Gamma(N-1)} dr d\tilde{r} = 1 \quad (\text{A.2})$$

and

$$\begin{aligned} \beta_2 &= \int_0^\infty \int_0^\infty \frac{\tilde{r}^{N-2} e^{-\frac{r+\tilde{r}}{2}}}{2^N \Gamma(N-1)} \times \\ &Q_{N-1} \left( \frac{\mu}{\sqrt{1-\mu^2}} \sqrt{\frac{\gamma\tilde{r}}{\gamma+1}}, \frac{\mu}{\sqrt{1-\mu^2}} \sqrt{\frac{r}{\gamma+1}} \right) dr d\tilde{r} \\ &= 1 - \left( \frac{\mu^2}{\gamma+1} \right)^{N-1}. \end{aligned} \quad (\text{A.3})$$

Afterwards,  $\beta_3$  can be formulated as (A.4) (see top of next page). By applying the results in [46, eq. (6.643.2)], the outer integral on  $r$  is evaluated and (a) is derived, where  $M_{u,v}(\cdot)$  is the Whittaker function. To evaluate the inner integral on  $\tilde{r}$ , we exploit an important connection between Whittaker functions  $M_{u,v}(\cdot)$  and generalized hypergeometric functions  ${}_aF_b(\cdot; \cdot; \cdot)$  established in [46, eq. (9.220.2)]. By leveraging the expansion for confluent hypergeometric function, (b) is obtained after simplifications. Then by applying the result in [46, eq. (3.326.2)] and after simplifications, (c) is obtained. As a result, the operation  $[\cdot]^+$  is adopted to guarantee positivity of the approximated expression, which proves Theorem 1.

### APPENDIX B PROOF OF THEOREM 2

First of all, we define  $\tilde{r}_1 = (x_0^{(i,i)})^2 + (y_0^{(i,i)})^2$ ,  $\tilde{r}_2 = \sum_{m \neq i}^N (x_0^{(m,i)})^2 + (y_0^{(m,i)})^2$ , which are central chi-square distributed with 2 degrees of freedom and  $2(N-1)$  degrees of freedom, respectively. Hence, the probability density function (PDF) of  $\tilde{r}_1$  and  $\tilde{r}_2$  is expressed as

$$f_{\tilde{r}_1}(r_1) = \frac{1}{2} \exp\left(-\frac{r_1}{2}\right), \quad (\text{B.1})$$

$$f_{\tilde{r}_2}(r_2) = \frac{r_2^{N-2} \exp\left(-\frac{r_2}{2}\right)}{2^{N-1} \Gamma(N-1)}. \quad (\text{B.2})$$

Then we define  $\mathcal{A} = \arg \max_{n \neq k^*} \frac{X_n}{Y_n}$ . Now, our objective is to derive the outage probability as  $\text{Prob}(Y_{k^*} \mathcal{A} < X_{k^*} < \hat{Q}_{\text{th}} - Y_{k^*})$ . In order to derive the WET outage probability with the WDT oriented strategy, the distribution of  $\mathcal{A}$  and  $X_{k^*}$  should firstly be formulated, respectively. The CDF of  $\mathcal{A}$  conditioned on  $\tilde{r}_1$  and  $\tilde{r}_2$  is given by [33, eq. (62)]

$$\begin{aligned} &F_{\mathcal{A}|\tilde{r}_1, \tilde{r}_2}(z) \\ &= \text{Prob} \left( \mathcal{A} = \arg \max_{n \neq k^*} \frac{X_n}{Y_n} < z \right) \\ &= \left[ 1 - \frac{1}{2} \int_0^\infty Q_1 \left( \sqrt{\frac{\mu^2}{1-\mu^2}} \sqrt{r_1}, \sqrt{zy} \right) \left( \frac{y}{\frac{\mu^2}{1-\mu^2} r_2} \right)^{\frac{N-2}{2}} \right. \\ &\quad \left. \times \exp \left( -\frac{y + \frac{\mu^2}{1-\mu^2} r_2}{2} \right) I_{N-2} \left( \sqrt{\frac{\mu^2}{1-\mu^2} r_2 y} \right) dy \right]^{K-1}. \end{aligned} \quad (\text{B.3})$$

$$\begin{aligned}
\beta_3 &= \left(\frac{1}{\gamma+1}\right)^{N-1} \sum_{k=0}^{N-2} \sum_{j=0}^{N-k-2} (\gamma+1)^k \gamma^{\frac{j-k}{2}} \frac{(N-(j+k)-1)_j}{j!} \times \\
&\int_0^\infty \int_0^\infty \frac{\tilde{r}^{N-2}}{2^N \Gamma(N-1)} e^{-\frac{r+\tilde{r}}{2}} \exp\left[-\frac{\mu^2}{2(1-\mu^2)} \left(\frac{\gamma\tilde{r}+r}{\gamma+1}\right)\right] \left(\frac{r}{\tilde{r}}\right)^{\frac{j+k}{2}} I_{j+k} \left(\frac{\mu^2}{1-\mu^2} \frac{\sqrt{\gamma r \tilde{r}}}{\gamma+1}\right) dr d\tilde{r} \\
&= \left(\frac{1}{\gamma+1}\right)^{N-1} \sum_{k=0}^{N-2} \sum_{j=0}^{N-k-2} (\gamma+1)^k \gamma^{\frac{j-k}{2}} \frac{(N-(j+k)-1)_j}{j!} \int_0^\infty \frac{\tilde{r}^{N-2-\frac{j+k}{2}}}{2^N \Gamma(N-1)} \exp\left[-\frac{1-\mu^2+\gamma}{2(1-\mu^2)(\gamma+1)} \tilde{r}\right] \tilde{r} d\tilde{r} \\
&\int_0^\infty r^{\frac{j+k}{2}} \exp\left[-\frac{(1-\mu^2)\gamma+1}{2(1-\mu^2)(\gamma+1)} r\right] I_{j+k} \left(\frac{\mu^2}{1-\mu^2} \frac{\sqrt{\gamma r}}{\gamma+1} \sqrt{r}\right) dr \\
&\stackrel{(a)}{=} \left(\frac{1}{\gamma+1}\right)^{N-1} \sum_{k=0}^{N-2} \sum_{j=0}^{N-k-2} (\gamma+1)^k \gamma^{\frac{j-k}{2}} \frac{(N-(j+k)-1)_j}{j!} \int_0^\infty \frac{\tilde{r}^{N-2-\frac{j+k}{2}}}{2^N \Gamma(N-1)} \exp\left[-\frac{1-\mu^2+\gamma}{2(1-\mu^2)(\gamma+1)} \tilde{r}\right] \tilde{r} d\tilde{r} \\
&\frac{2(1-\mu^2)(\gamma+1)}{\mu^2 \sqrt{\gamma \tilde{r}}} e^{\frac{\mu^4 \gamma \tilde{r}}{4(1-\mu^2)(\gamma+1)[(1-\mu^2)\gamma+1]}} \left[\frac{(1-\mu^2)\gamma+1}{2(1-\mu^2)(\gamma+1)}\right]^{-\frac{j+k+1}{2}} M_{-\frac{j+k+1}{2}, \frac{j+k}{2}} \left(\frac{\mu^4 \gamma \tilde{r}}{2(1-\mu^2)(\gamma+1)[(1-\mu^2)\gamma+1]}\right) \\
&\stackrel{(b)}{=} \left[\frac{\mu^4 \gamma}{(1-\mu^2)\gamma+1}\right]^{\frac{j+k+1}{2}} \frac{2(1-\mu^2)(\gamma+1)}{\mu^2 \sqrt{\gamma}} [(1-\mu^2)\gamma+1]^{-\frac{j+k+1}{2}} \times \\
&\int_0^\infty \frac{\tilde{r}^{N-2}}{2^N \Gamma(N-1)} \exp\left[-\left(\frac{1-\mu^2+\gamma}{2(1-\mu^2)(\gamma+1)} + \frac{\mu^4 \gamma}{4((1-\mu^2)\gamma+1)(1-\mu^2)(\gamma+1)}\right) \tilde{r}\right] d\tilde{r} \\
&\stackrel{(c)}{=} \left[\frac{2\gamma(1-\mu^2)+1}{2\gamma^2+(3-\mu^2)\gamma+1}\right]^{N-1} (1-\mu^2) \sum_{k=0}^{N-2} \sum_{j=0}^{N-k-2} (\gamma+1)^{k+1} \gamma^j \frac{(N-(j+k)-1)_j}{j!} \mu^{2(j+k)} [(1-\mu^2)\gamma+1]^{-j-k-1}
\end{aligned} \tag{A.4}$$

By differentiating the CDF of  $\mathcal{A}$ , the PDF of  $\mathcal{A}$  conditioned on  $\tilde{r}_1$  and  $\tilde{r}_2$  is obtained as

$$\begin{aligned}
&f_{\mathcal{A}|\tilde{r}_1, \tilde{r}_2}(z) \\
&= \frac{\partial F_{\mathcal{A}|\tilde{r}_1, \tilde{r}_2}(z)}{\partial z} \\
&= (K-1) \left[1 - \frac{1}{2} \int_0^\infty Q_1 \left(\sqrt{\frac{\mu^2}{1-\mu^2}} r_1, \sqrt{zy}\right) \times \right. \\
&\quad \left. e^{-\frac{y+\frac{\mu^2}{1-\mu^2} r_2}{2}} I_{N-2} \left(\sqrt{\frac{\mu^2}{1-\mu^2}} \sqrt{r_2 y}\right) dy\right]^{K-2} \\
&\times \int_0^\infty \frac{y}{2} e^{-\frac{\mu^2}{1-\mu^2} r_1 + zy} I_0 \left(\sqrt{\frac{\mu^2}{1-\mu^2}} r_1 zy\right) \times \\
&\quad \frac{1}{2} \left(\frac{y}{\frac{\mu^2}{1-\mu^2} r_2}\right)^{\frac{N-2}{2}} e^{-\frac{y+\frac{\mu^2}{1-\mu^2} r_2}{2}} I_{N-2} \left(\sqrt{\frac{\mu^2}{1-\mu^2}} r_2 y\right) dy.
\end{aligned} \tag{B.4}$$

By applying the results in [33, eq. (59)], the CDF of  $X_{k^*}$  conditioned on  $\tilde{r}_1$  is obtained as

$$F_{X_{k^*}|\tilde{r}_1}(t) = \left[1 - Q_1 \left(\sqrt{\frac{\mu^2}{1-\mu^2}} r_1, \sqrt{t}\right)\right]. \tag{B.5}$$

Further, by applying the results in [33, eq. (61)], the PDF of  $Y_{k^*}$  conditioned on  $\tilde{r}_2$  is obtained as by substituting the

variable  $K = 1$  is obtained as

$$\begin{aligned}
f_{Y_{k^*}|\tilde{r}_2}(y) &= \frac{1}{2} \left(\frac{(1-\mu^2)y}{\mu^2 r_2}\right)^{\frac{N-2}{2}} e^{-\frac{y+\frac{\mu^2}{1-\mu^2} r_2}{2}} \\
&\quad \times I_{N-2} \left(\sqrt{\frac{\mu^2}{1-\mu^2}} r_2 y\right) dr_2.
\end{aligned} \tag{B.6}$$

As a consequence, the probability  $\text{Prob}(Y_{k^*} \mathcal{A} < X_{k^*} < \hat{Q}_{\text{th}} - Y_{k^*})$  is then re-formulated as (B.7) (see top of next page), where (a) accounts for the fact that  $X_{k^*}$ ,  $Y_{k^*}$  and  $\mathcal{A}$  are independent when conditioned on  $\tilde{r}_1$  and  $\tilde{r}_2$ , (b) is derived with the results of PDF of  $\tilde{r}_1$  and  $\tilde{r}_2$ . Finally, the desired result (19) is obtained by applying the results in (B.4), (B.5) and (B.6), which finally proves Theorem 2.

#### APPENDIX C PROOF OF THEOREM 3

When  $\hat{Q}_{\text{th}}$  becomes larger or  $N$  gets smaller, the Marcum- $Q$  function  $Q_N \left(\sqrt{\frac{\mu^2}{1-\mu^2}} r, \sqrt{\hat{Q}_{\text{th}}}\right)$  goes to zero. Hence, the binomial approximation can be applied as

$$\begin{aligned}
&\left[1 - Q_N \left(\sqrt{\frac{\mu^2 r}{1-\mu^2}}, \sqrt{\hat{Q}_{\text{th}}}\right)\right]^K \\
&\quad \approx 1 - K Q_N \left(\sqrt{\frac{\mu^2 r}{1-\mu^2}}, \sqrt{\hat{Q}_{\text{th}}}\right).
\end{aligned} \tag{C.1}$$

$$\begin{aligned}
& \text{Prob} \left( Y_{k^*} \max_{n \neq k^*} \frac{X_n}{Y_n} < X_{k^*} < \widehat{Q}_{\text{th}} - Y_{k^*} \right) = \text{Prob}(Y_{k^*} \mathcal{A} < X_{k^*} < \widehat{Q}_{\text{th}} - Y_{k^*}) \\
& \stackrel{(a)}{=} \int_{z=0}^{\infty} \int_{y=0}^{\widehat{Q}_{\text{th}} - z} \text{Prob}(Y_{k^*} \mathcal{A} < X_{k^*} < \widehat{Q}_{\text{th}} - Y_{k^*} | Y_{k^*}, \mathcal{A}) f_{Y_{k^*}}(y) f_{\mathcal{A}}(z) dy dz \\
& \stackrel{(b)}{=} \int_{r_1=0}^{\infty} \int_{r_2=0}^{\infty} \int_{z=0}^{\infty} \int_{y=0}^{\widehat{Q}_{\text{th}} - z} \underbrace{\frac{r_2^{N-2} \exp\left(-\frac{r_1+r_2}{2}\right)}{2^N \Gamma(N-1)}}_{f_{\tilde{r}_1}(r_1) f_{\tilde{r}_2}(r_2)} \left[ F_{X_{k^*} | \tilde{r}_1}(\widehat{Q}_{\text{th}} - y) - F_{X_{k^*} | \tilde{r}_1}(yz) \right] f_{Y_{k^*} | \tilde{r}_2}(y) f_{\mathcal{A} | \tilde{r}_1, \tilde{r}_2}(z) dy dz dr_1 dr_2
\end{aligned} \tag{B.7}$$

Then the exact WET outage probability with the WET oriented strategy for maximizing the EHP in (22) is approximated as

$$\begin{aligned}
& \epsilon_{\text{WET-EHP}}^i \\
& \approx \int_0^{\infty} \frac{r^{N-1} \exp\left(-\frac{r}{2}\right)}{2^N \Gamma(N)} \left[ 1 - K Q_N \left( \sqrt{\frac{\mu^2 r}{1-\mu^2}}, \sqrt{\widehat{Q}_{\text{th}}} \right) \right] dr \\
& = 1 - K \int_0^{\infty} \frac{r^{N-1} \exp\left(-\frac{r}{2}\right)}{2^N \Gamma(N)} Q_N \left( \sqrt{\frac{\mu^2 r}{1-\mu^2}}, \sqrt{\widehat{Q}_{\text{th}}} \right) dr.
\end{aligned} \tag{C.2}$$

By applying the results in [48], a closed-form solution for the following type of integral is available, i.e.,

$$\mathcal{F}(k, m, a, b, p) = \int_0^{\infty} x^{k-1} Q_m(a\sqrt{x}, b) e^{-px} dx. \tag{C.3}$$

By using the result in [48, eq. (12)] to evaluate the integral  $\mathcal{F}\left(N, N, \sqrt{\frac{\mu^2}{1-\mu^2}}, \sqrt{\widehat{Q}_{\text{th}}}, \frac{1}{2}\right)$ , and adopting the operation  $[\cdot]^+$  to guarantee positivity of the approximated expression, the approximated WET outage probability with the WET oriented strategy is obtained in (23), which proves Theorem 3.

#### APPENDIX D PROOF OF THEOREM 4

We define  $\mathcal{B} = \arg \max_{n \neq k^*} X_n + Y_n$ , where  $k^*$  is the optimal port. Now, our objective is to derive the outage probability as  $\text{Prob}(\mathcal{B} - Y_{k^*} < X_{k^*} < \gamma Y_{k^*})$ , where the PDF of  $X_{k^*}$  and the distribution of  $\mathcal{B}$  should be firstly formulated. By applying the results in [33, eq. (58)], the unconditioned PDF of  $X_{k^*}$  by substituting  $K = 1$  is given by

$$\begin{aligned}
& f_{X_{k^*}}(t) \\
& = \int_0^{\infty} \underbrace{\frac{\exp\left(-\frac{r_1}{2}\right)}{2}}_{f_{\tilde{r}_1}(r_1)} \frac{e^{-\frac{\mu^2}{2} r_1 + t}}{2} I_0 \left( \sqrt{\frac{\mu^2}{1-\mu^2}} r_1 t \right) dr_1.
\end{aligned} \tag{D.1}$$

Similarly, the PDF  $f_{\mathcal{B}}(z)$  of  $\mathcal{B}$  conditioned on  $\tilde{r}_1$  and  $\tilde{r}_2$  can be formulated using [43, eq. (26)], while the CDF of  $\mathcal{B}$  conditioned on  $\tilde{r}_1$  and  $\tilde{r}_2$  is formulated as [43, eq. (19)]

$$F_{\mathcal{B} | \tilde{r}_1, \tilde{r}_2}(z) = \left[ 1 - Q_N \left( \sqrt{\frac{\mu^2}{1-\mu^2}} (r_1 + r_2), \sqrt{z} \right) \right]^{K-1}. \tag{D.2}$$

Then, the probability  $\text{Prob}(\mathcal{B} - Y_{k^*} < X_{k^*} < \gamma Y_{k^*})$  is evaluated by (D.3) (see top of next page), where (a) accounts for the fact that  $X_{k^*}$ ,  $Y_{k^*}$  and  $\mathcal{B}$  are independent when conditioned on  $\tilde{r}_1$  and  $\tilde{r}_2$ , (b) is derived by using the PDF of  $\tilde{r}_1$  and  $\tilde{r}_2$ , (c) is obtained by integrating  $z$  by parts and subsequent simplification. Then, (25) is achieved by applying the results in (B.6), (D.1) and (D.2), which finally proves Theorem 4.

#### APPENDIX E PROOF OF THEOREM 5

Note that  $X_1, \dots, X_K$  are all independent with each other when conditioned on  $\tilde{r}_1$ , which follows chi-square distribution with 2 degrees of freedom. Hence, we can get the joint PDF of  $X_1, \dots, X_K$  as [33, eq. (58)]

$$\begin{aligned}
& f_{X_1, \dots, X_K}(t_1, \dots, t_K) = \int_0^{\infty} \underbrace{\frac{\exp\left(-\frac{r_1}{2}\right)}{2}}_{f_{\tilde{r}_1}(r_1)} \times \\
& \prod_{k=1}^K \frac{1}{2} e^{-\frac{t_k + \frac{\mu^2}{2} r_1}{2}} I_0 \left( \sqrt{\frac{\mu^2}{1-\mu^2}} \sqrt{r_1 t_k} \right) dr_1.
\end{aligned} \tag{E.1}$$

Similarly,  $Y_1, \dots, Y_K$  are all independent with each other when conditioned on  $\tilde{r}_2$ , which follows chi-square distribution with  $2(N-1)$  degrees of freedom. Then we can get the joint CDF of  $Y_1, \dots, Y_K$  as [43, eq. (17)]

$$\begin{aligned}
& F_{Y_1, \dots, Y_K}(t_1, \dots, t_K) = \int_0^{\infty} \underbrace{\frac{r_2^{N-2} \exp\left(-\frac{r_2}{2}\right)}{2^{N-1} \Gamma(N-1)}}_{f_{\tilde{r}_2}(r_2)} \times \\
& \prod_{k=1}^K \left[ 1 - Q_{N-1} \left( \sqrt{\frac{\mu^2}{1-\mu^2}} r_2, \sqrt{t_k} \right) \right] dr_2.
\end{aligned} \tag{E.2}$$

Further, the special IDET outage probability  $\text{Prob}(\text{SINR}_k^i < \gamma, Q_k^i < Q_{\text{th}}), \forall k = 1, 2, \dots, K$  is evaluated by (E.3) (see next page). Note that (a) accounts for the fact that  $X_k$  and  $Y_k$  ( $k = 1, \dots, K$ ) are independent when conditioned on  $\tilde{r}_1$  and  $\tilde{r}_2$ , (b) is derived according to (E.1) and (E.2), and (c) moves the integration over  $X_k$  inside the product. Finally, (29) is achieved and then the proof of Theorem 5 ends.

#### APPENDIX F PROOF OF COROLLARY 3

First, for WDT, according to (15) and (16), we can obtain (F.1) (see next page), where (a) accounts for the fact that for



$\text{Prob}(\mathcal{B} - Y_{k^*} < X_{k^*} < \gamma Y_{k^*})$

$$\begin{aligned}
&\stackrel{(a)}{=} \int_{y=0}^{\infty} \int_{z=0}^{(1+\gamma)y} \text{Prob}(\mathcal{B} - Y_{k^*} < X_{k^*} < \gamma Y_{k^*} | Y_{k^*}, \mathcal{B}) f_{Y_{k^*}}(y) f_{\mathcal{B}}(z) dy dz \\
&\stackrel{(b)}{=} \int_{r_1=0}^{\infty} \int_{r_2=0}^{\infty} \int_{y=0}^{\infty} \int_{z=0}^{(1+\gamma)y} \underbrace{\frac{r_2^{N-2} \exp\left(-\frac{r_1+r_2}{2}\right)}{2^N \Gamma(N-1)}}_{f_{\tilde{r}_1}(r_1) f_{\tilde{r}_2}(r_2)} [F_{X_{k^*} | \tilde{r}_1}(\gamma y) - F_{X_{k^*} | \tilde{r}_1}(z - y)] f_{Y_{k^*} | \tilde{r}_2}(y) f_{\mathcal{B} | \tilde{r}_1, \tilde{r}_2}(z) dy dz dr_1 dr_2 \quad (\text{D.3}) \\
&\stackrel{(c)}{=} \int_{r_1=0}^{\infty} \int_{r_2=0}^{\infty} \int_{y=0}^{\infty} \int_{t=0}^{\gamma y} \underbrace{\frac{r_2^{N-2} \exp\left(-\frac{r_1+r_2}{2}\right)}{2^N \Gamma(N-1)}}_{f_{\tilde{r}_1}(r_1) f_{\tilde{r}_2}(r_2)} F_{\mathcal{B} | \tilde{r}_1, \tilde{r}_2}(t + y) f_{X_{k^*}}(t) f_{Y_{k^*}}(y) dt dy dr_1 dr_2
\end{aligned}$$

$\text{Prob}(\text{SINR}_k^i < \gamma, Q_k^i < Q_{\text{th}}), \forall k = 1, 2, \dots, K$

$$\begin{aligned}
&= \text{Prob}\left(\frac{X_1}{\gamma} < Y_1 < \widehat{Q}_{\text{th}} - X_1, \dots, \frac{X_K}{\gamma} < Y_K < \widehat{Q}_{\text{th}} - X_K\right) \\
&= \int \dots \int \text{Prob}\left(\frac{X_1}{\gamma} < Y_1 < \widehat{Q}_{\text{th}} - X_1, \dots, \frac{X_K}{\gamma} < Y_K < \widehat{Q}_{\text{th}} - X_K \mid X_1, \dots, X_K\right) f_{X_1, \dots, X_K}(x_1, \dots, x_K) dx_1 \dots dx_K \\
&\stackrel{(a)}{=} \underbrace{\int_0^{\frac{\widehat{Q}_{\text{th}}}{(1+1/\gamma)}} \dots \int_0^{\frac{\widehat{Q}_{\text{th}}}{(1+1/\gamma)}}}_{x_1, \dots, x_K} \left[ F_{Y_1, \dots, Y_K}(\widehat{Q}_{\text{th}} - x_1, \dots, \widehat{Q}_{\text{th}} - x_K) - F_{Y_1, \dots, Y_K}\left(\frac{x_1}{\gamma}, \dots, \frac{x_K}{\gamma}\right) \right] f_{X_1, \dots, X_K}(x_1, \dots, x_K) dx_1 \dots dx_K \\
&\stackrel{(b)}{=} \underbrace{\int_0^{\frac{\widehat{Q}_{\text{th}}}{(1+1/\gamma)}} \dots \int_0^{\frac{\widehat{Q}_{\text{th}}}{(1+1/\gamma)}}}_{x_1, \dots, x_K} \int_{r_1=0}^{\infty} \int_{r_2=0}^{\infty} \frac{r_2^{N-2} \exp\left(-\frac{r_1+r_2}{2}\right)}{2^N \Gamma(N-1)} \\
&\quad \times \prod_{k=1}^K \left[ Q_{N-1}\left(\sqrt{\frac{\mu^2}{1-\mu^2}} r_1, \sqrt{\frac{x_k}{\gamma}}\right) - Q_{N-1}\left(\sqrt{\frac{\mu^2}{1-\mu^2}} r_1, \sqrt{\widehat{Q}_{\text{th}} - x_k}\right) \right] \\
&\quad \times \frac{1}{2} e^{-\frac{x_k + \frac{\mu^2}{1-\mu^2} r_2}{2}} I_0\left(\sqrt{\frac{\mu^2}{1-\mu^2}} \sqrt{r_2 x_k}\right) dr_1 dr_2 dx_1 \dots dx_K \\
&\stackrel{(c)}{=} \int_{r_1=0}^{\infty} \int_{r_2=0}^{\infty} \frac{r_2^{N-2} \exp\left(-\frac{r_1+r_2}{2}\right)}{2^N \Gamma(N-1)} \prod_{k=1}^K \int_{x_k=0}^{\frac{\widehat{Q}_{\text{th}}}{(1+1/\gamma)}} \left[ Q_{N-1}\left(\sqrt{\frac{\mu^2}{1-\mu^2}} r_1, \sqrt{\frac{x_k}{\gamma}}\right) - Q_{N-1}\left(\sqrt{\frac{\mu^2}{1-\mu^2}} r_1, \sqrt{\widehat{Q}_{\text{th}} - x_k}\right) \right] \\
&\quad \times \frac{1}{2} e^{-\frac{x_k + \frac{\mu^2}{1-\mu^2} r_2}{2}} I_0\left(\sqrt{\frac{\mu^2}{1-\mu^2}} \sqrt{r_2 x_k}\right) dx_k dr_1 dr_2 \quad (\text{E.3})
\end{aligned}$$

$$\begin{aligned}
\mathcal{C} &= \left[ \frac{2(1-\mu^2)\gamma + 1}{2\gamma^2 + (3-\mu^2)\gamma + 1} \right]^{N-1} (1-\mu^2) \sum_{k=0}^{N-2} \sum_{j=0}^{N-k-2} (\gamma+1)^{k+1} \gamma^j \frac{(N-j-k-1)_j}{j!} \mu^{2(j+k)} ((1-\mu^2)\gamma + 1)^{-j-k-1} \\
&\stackrel{(a)}{<} \left( \frac{1-\mu^2}{\gamma} \right)^{N-1} \sum_{k=0}^{N-2} \sum_{j=0}^{N-k-2} \frac{(N-j-k-1)_j}{j!} \left( \frac{\mu^2}{1-\mu^2} \right)^{j+k} \left( \frac{\gamma+1}{\gamma + \frac{1}{1-\mu^2}} \right)^{j+k+1} \\
&\stackrel{(b)}{<} \left( \frac{1-\mu^2}{\gamma} \right)^{N-1} \sum_{k=0}^{N-2} \sum_{j=0}^{N-k-2} \frac{(N-j-k-1)_j}{j!} \left( \frac{\mu^2}{1-\mu^2} \right)^{j+k} \\
&\stackrel{(c)}{\approx} \left( \frac{1-\mu^2}{\gamma} \right)^{N-1}
\end{aligned} \quad (\text{E.1})$$

$$\begin{aligned}
\epsilon_{\text{WET-EHP}}^i &\approx \left[ 1 - K \frac{\Gamma\left(N, \frac{\widehat{Q}_{\text{th}}}{2}\right)}{\Gamma(N)} - K \frac{\mu^2 \left(\frac{\widehat{Q}_{\text{th}}}{2}\right)^N \exp\left(-\frac{\widehat{Q}_{\text{th}}}{2}\right)}{N!} \sum_{l=0}^{N-1} (1-\mu^2)^l {}_1F_1\left(l+1; N+1; \frac{\mu^2 \widehat{Q}_{\text{th}}}{2}\right) \right]^+ \\
&\stackrel{(a)}{>} 1 - K \frac{\Gamma\left(N, \frac{\widehat{Q}_{\text{th}}}{2}\right)}{\Gamma(N)} - K \frac{\mu^2 \left(\frac{\widehat{Q}_{\text{th}}}{2}\right)^N \exp\left(-\frac{\widehat{Q}_{\text{th}}}{2}(1-\mu^2)\right)}{N!} \sum_{l=0}^{N-1} (1-\mu^2)^l \\
&\stackrel{(b)}{=} \left[ 1 - K \frac{\Gamma\left(N, \frac{\widehat{Q}_{\text{th}}}{2}\right)}{\Gamma(N)} - K \frac{(1-(1-\mu^2)^N) \left(\frac{\widehat{Q}_{\text{th}}}{2}\right)^N \exp\left(-\frac{\widehat{Q}_{\text{th}}}{2}(1-\mu^2)\right)}{N!} \right]^+ \\
&\stackrel{(c)}{\approx} \left[ 1 - K \frac{\Gamma\left(N, \frac{\widehat{Q}_{\text{th}}}{2}\right)}{\Gamma(N)} \right]^+ \\
&\stackrel{(d)}{=} \left[ 1 - K \exp\left(-\frac{\widehat{Q}_{\text{th}}}{2}\right) \sum_{s=0}^N \frac{\left(\frac{\widehat{Q}_{\text{th}}}{2}\right)^s}{s!} \right]^+
\end{aligned} \tag{F.3}$$

small  $\mu$ , that  $\frac{2(1-\mu^2)\gamma+1}{2\gamma^2+(3-\mu^2)\gamma+1} < \frac{1-\mu^2}{\gamma}$ , (b) accounts for the fact that for small  $\mu$ ,  $1-\mu^2 \approx 1$ , and (c) ignores the higher-order terms which get smaller. As a result, we have

$$\epsilon_{\text{WDT-SINR}}^i > \left[ 1 - K \left(\frac{\mu^2}{\gamma+1}\right)^{N-1} - K \left(\frac{1-\mu^2}{\gamma}\right)^{N-1} \right]^+ . \tag{F.2}$$

Therefore, for large  $N$ , the second term and the third term of (F.2) are close to 0, which means that the lower bound of WDT outage probability is close to 1. Thus, the WDT outage probability  $\epsilon_{\text{WDT-SINR}}^i$  will be close to 1 for large  $N$ .

As for WET, (23) can be lower bounded by (F.3) (see top of this page), where (a) accounts for the fact that [49, eq. (13.6.1)]

$$\begin{aligned}
{}_1F_1\left(l; N+1; \frac{\mu^2 \widehat{Q}_{\text{th}}}{2}\right) &< {}_1F_1\left(N+1; N+1; \frac{\mu^2 \widehat{Q}_{\text{th}}}{2}\right) \\
&= \exp\left(\frac{\mu^2 \widehat{Q}_{\text{th}}}{2}\right), \quad \forall l,
\end{aligned} \tag{F.4}$$

(b) makes some simplifications, (c) accounts for the fact that when  $\mu$  is small,  $1-\mu^2 \approx 1$ ; hence the third term can be omitted, and (d) applies the result of [49, eq. (8.4.10)]. As can be seen, the lower bound is a strictly decreasing function of  $N$ . Evidently, when  $N$  is small, the lower bound in (F.3) is close to 1. Thus, the WET outage probability  $\epsilon_{\text{WET-EHP}}^i$  will be close to 1 for small  $N$ .

## REFERENCES

- [1] B. Zong *et al.*, "6G technologies: Key drivers, core requirements, system architectures, and enabling technologies," *IEEE Veh. Tech. Mag.*, vol. 14, no. 3, pp. 18–27, Sept. 2019.
- [2] C.-X. Wang *et al.*, "On the road to 6G: Visions, requirements, key technologies, and testbeds," *IEEE Commun. Surveys Tuts.*, vol. 25, no. 2, pp. 905–974, Secondquarter 2023.
- [3] K. W. Choi *et al.*, "Distributed wireless power transfer system for internet of things devices," *IEEE Internet Things J.*, vol. 5, no. 4, pp. 2657–2671, Aug. 2018.
- [4] L. R. Varshney, "Transporting information and energy simultaneously," in *Proc. IEEE Inter. Symp. Inf. Theory (ISIT)*, pp. 1612–1616, 6–11 Jul. 2008, Toronto, ON, Canada.
- [5] R. Zhang and C. K. Ho, "MIMO broadcasting for simultaneous wireless information and power transfer," *IEEE Trans. Wireless Commun.*, vol. 12, no. 5, pp. 1989–2001, May 2013.
- [6] I. Krikidis *et al.*, "Simultaneous wireless information and power transfer in modern communication systems," *IEEE Commun. Mag.*, vol. 52, no. 11, pp. 104–110, Nov. 2014.
- [7] V. Khodamoradi, A. Sali, O. Messadi, A. Khalili, and B. B. M. Ali, "Energy-efficient massive MIMO SWIPT-enabled systems," *IEEE Trans. Veh. Tech.*, vol. 71, no. 5, pp. 5111–5127, May 2022.
- [8] G. Yang, C. K. Ho, R. Zhang, and Y. L. Guan, "Throughput optimization for massive MIMO systems powered by wireless energy transfer," *IEEE J. Sel. Areas Commun.*, vol. 33, no. 8, pp. 1640–1650, Aug. 2015.
- [9] K. K. Wong, K. F. Tong, Y. Shen, Y. Chen, and Y. Zhang, "Bruce Lee-inspired fluid antenna system: Six research topics and the potentials for 6G," *Frontiers Commun. and Netw., section Wireless Commun.*, vol. 3, no. 853416, Mar. 2022.
- [10] K.-K. Wong, W. K. New, X. Hao, K.-F. Tong, and C.-B. Chae, "Fluid antenna system—part I: Preliminaries," *IEEE Commun. Lett.*, vol. 27, no. 8, pp. 1919–1923, Aug. 2023.
- [11] Y. Shen *et al.*, "Design and implementation of mmWave surface wave enabled fluid antennas and experimental results for fluid antenna multiple access," *arXiv preprint, arXiv:2405.09663*, May 2024.
- [12] J. Zhang *et al.*, "A pixel-based reconfigurable antenna design for fluid antenna systems," *arXiv preprint, arXiv:2406.05499*, Jun. 2024.
- [13] S. Zargari, A. Khalili, and R. Zhang, "Energy efficiency maximization via joint active and passive beamforming design for multiuser MISO IRS-aided SWIPT," *IEEE Wireless Commun. Lett.*, vol. 10, no. 3, pp. 557–561, Mar. 2021.
- [14] H. Lee, K.-J. Lee, H. Kim, and I. Lee, "Joint transceiver optimization for MISO SWIPT systems with time switching," *IEEE Trans. Wireless Commun.*, vol. 17, no. 5, pp. 3298–3312, May 2018.
- [15] R. R. Kurup and A. V. Babu, "Power adaptation for improving the performance of time switching SWIPT-based full-duplex cooperative NOMA network," *IEEE Commun. Lett.*, vol. 24, no. 12, pp. 2956–2960, Dec. 2020.
- [16] S. Timotheou, G. Zheng, C. Masouros, and I. Krikidis, "Exploiting constructive interference for simultaneous wireless information and power transfer in multiuser downlink systems," *IEEE J. Sel. Areas Commun.*, vol. 34, no. 5, pp. 1772–1784, May 2016.
- [17] S. Timotheou, I. Krikidis, G. Zheng, and B. Ottersten, "Beamforming for MISO interference channels with QoS and RF energy transfer," *IEEE Trans. Wireless Commun.*, vol. 13, no. 5, pp. 2646–2658, May 2014.
- [18] A. A. Nasir, H. D. Tuan, D. T. Ngo, T. Q. Duong, and H. V. Poor, "Beamforming design for wireless information and power transfer

- systems: Receive power-splitting versus transmit time-switching," *IEEE Trans. Commun.*, vol. 65, no. 2, pp. 876–889, Feb. 2017.
- [19] Y. Zhao, Y. Wu, J. Hu, and K. Yang, "Time-index modulation for integrated data and energy transfer: A remedy for time switching," *IEEE Wireless Commun. Lett.*, vol. 11, no. 9, pp. 1815–1819, Sept. 2022.
- [20] Y. Zhao, Y. Wu, J. Hu, and K. Yang, "A general analysis and optimization framework of time index modulation for integrated data and energy transfer," *IEEE Trans. Wireless Commun.*, vol. 22, no. 6, pp. 3657–3670, Jun. 2023.
- [21] K. K. Wong, A. Shojaeifard, K.-F. Tong, and Y. Zhang, "Performance limits of fluid antenna systems," *IEEE Commun. Lett.*, vol. 24, no. 11, pp. 2469–2472, Nov. 2020.
- [22] K.-K. Wong, A. Shojaeifard, K.-F. Tong, and Y. Zhang, "Fluid antenna systems," *IEEE Trans. Wireless Commun.*, vol. 20, no. 3, pp. 1950–1962, Mar. 2021.
- [23] M. Khammassi, A. Kammoun, and M.-S. Alouini, "A new analytical approximation of the fluid antenna system channel," *IEEE Trans. Wireless Commun.*, vol. 22, no. 12, pp. 8843–8858, Dec. 2023.
- [24] W. K. New, K.-K. Wong, H. Xu, K.-F. Tong, and C.-B. Chae, "Fluid antenna system: New insights on outage probability and diversity gain," *IEEE Trans. Wireless Commun.*, vol. 23, no. 1, pp. 128–140, Jan. 2024.
- [25] C. Psomas, G. M. Kraidy, K.-K. Wong, and I. Krikidis, "On the diversity and coded modulation design of fluid antenna systems," *IEEE Trans. Wireless Commun.*, vol. 23, no. 3, pp. 2082–2096, Mar. 2024.
- [26] J. D. Vega-Sánchez, A. E. López-Ramírez, L. Urquiza-Aguiar and D. P. M. Osorio, "Novel expressions for the outage probability and diversity gains in fluid antenna system," *IEEE Wireless Commun. Lett.*, vol. 13, no. 2, pp. 372–376, Feb. 2024.
- [27] J. D. Vega-Sánchez, L. Urquiza-Aguiar, M. C. P. Paredes and D. P. M. Osorio, "A simple method for the performance analysis of fluid antenna systems under correlated Nakagami- $m$  fading," *IEEE Wireless Commun. Lett.*, vol. 13, no. 2, pp. 377–381, Feb. 2024.
- [28] P. D. Alvim *et al.*, "On the performance of fluid antennas systems under  $\alpha$ - $\mu$  fading channels," *IEEE Wireless Commun. Lett.*, vol. 13, no. 1, pp. 108–112, Jan. 2024.
- [29] C. Psomas, P. J. Smith, H. A. Suraweera and I. Krikidis, "Continuous fluid antenna systems: Modeling and analysis," *IEEE Commun. Lett.*, vol. 27, no. 12, pp. 3370–3374, Dec. 2023.
- [30] W. K. New, K. K. Wong, H. Xu, K. F. Tong and C.-B. Chae, "An information-theoretic characterization of MIMO-FAS: Optimization, diversity-multiplexing tradeoff and  $q$ -outage capacity," *IEEE Trans. Wireless Commun.*, vol. 23, no. 6, pp. 5541–5556, Jun. 2024.
- [31] K.-K. Wong and K.-F. Tong, "Fluid antenna multiple access," *IEEE Trans. Wireless Commun.*, vol. 21, no. 7, pp. 4801–4815, Jul. 2022.
- [32] K.-K. Wong, K.-F. Tong, Y. Chen, and Y. Zhang, "Fast fluid antenna multiple access enabling massive connectivity," *IEEE Commun. Lett.*, vol. 27, no. 2, pp. 711–715, Feb. 2023.
- [33] K.-K. Wong, D. Morales-Jimenez, K.-F. Tong, and C.-B. Chae, "Slow fluid antenna multiple access," *IEEE Trans. Wireless Commun.*, vol. 71, no. 5, pp. 2831–2846, May 2023.
- [34] H. Xu *et al.*, "Revisiting outage probability analysis for two-user fluid antenna multiple access system," *IEEE Trans. Wireless Commun.*, early access, DOI:10.1109/TWC.2024.3363499, Feb. 2024.
- [35] H. Yang, K.-K. Wong, K.-F. Tong, Y. Zhang, and C.-B. Chae, "Performance analysis of slow fluid antenna multiple access in noisy channels using Gauss-Laguerre and Gauss-Hermite quadratures," *IEEE Commun. Lett.*, vol. 27, no. 7, pp. 1734–1738, Jul. 2023.
- [36] N. Waqar, K.-K. Wong, K.-F. Tong, A. Sharples, and Y. Zhang, "Deep learning enabled slow fluid antenna multiple access," *IEEE Commun. Lett.*, vol. 27, no. 3, pp. 861–865, Mar. 2023.
- [37] Y. Chen, S. Li, Y. Hou, and X. Tao, "Energy-efficiency optimization for slow fluid antenna multiple access using mean-field game," *IEEE Commun. Lett.*, vol. 13, no. 4, pp. 915–918, Apr. 2024.
- [38] K.-K. Wong, K.-F. Tong, Y. Chen, Y. Zhang, and C.-B. Chae, "Opportunistic fluid antenna multiple access," *IEEE Trans. Wireless Commun.*, vol. 22, no. 11, pp. 7819–7833, Nov. 2023.
- [39] C. Wang *et al.*, "Fluid antenna system liberating multiuser MIMO for ISAC via deep reinforcement learning," *IEEE Trans. Wireless Commun.*, early access, DOI:10.1109/TWC.2024.3376800, Mar. 2024.
- [40] F. Rostami Ghadi *et al.*, "Fluid antenna-assisted dirty multiple access channels over composite fading," *IEEE Commun. Lett.*, vol. 28, no. 2, pp. 382–386, Feb. 2024.
- [41] W. K. New *et al.*, "Fluid antenna system enhancing orthogonal and non-orthogonal multiple access," *IEEE Commun. Lett.*, vol. 28, no. 1, pp. 218–222, Jan. 2024.
- [42] L. Zhu, and K. K. Wong, "Historical review of fluid antennas and movable antennas," *arXiv preprint*, arXiv:2401.02362v2, Jan. 2024.
- [43] X. Lin, H. Yang, Y. Zhao, J. Hu, and K.-K. Wong, "Performance analysis of integrated data and energy transfer assisted by fluid antenna systems," in *Proc. IEEE Int. Conf. Commun. (ICC)*, pp. 1–6, 9–13 Jun. 2024, Denver, CO, USA.
- [44] Z. Zong *et al.*, "Optimal transceiver design for SWIPT in  $K$ -user MIMO interference channels," *IEEE Trans. Wireless Commun.*, vol. 15, no. 1, pp. 430–445, Jan. 2016.
- [45] M.-M. Zhao, Y. Cai, Q. Shi, M. Hong, and B. Champagne, "Joint transceiver designs for full-duplex  $K$ -pair MIMO interference channel with SWIPT," *IEEE Trans. Commun.*, vol. 65, no. 2, pp. 890–905, Feb. 2017.
- [46] I. S. Gradshteyn and I. M. Ryzhik, *Table of integrals, series, and products*. New York, NY, USA: Academic press, 2014.
- [47] R. Jiang *et al.*, "On the coverage of UAV-assisted SWIPT networks with nonlinear EH model," *IEEE Trans. Wireless Commun.*, vol. 21, no. 6, pp. 4464–4481, Jun. 2022.
- [48] P. C. Sofotasios, S. Muhaidat, G. K. Karagiannidis, and B. S. Sharif, "Solutions to integrals involving the Marcum  $Q$ -function and applications," *IEEE Signal Process. Lett.*, vol. 22, no. 10, pp. 1752–1756, Oct. 2015.
- [49] F. W. Olver, *NIST handbook of mathematical functions*. Cambridge University Press, 2010.